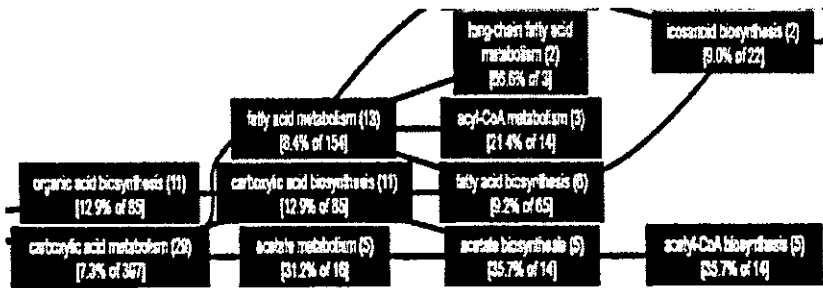
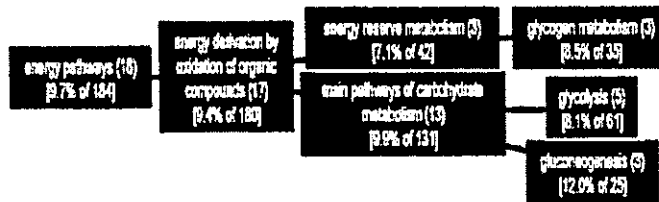
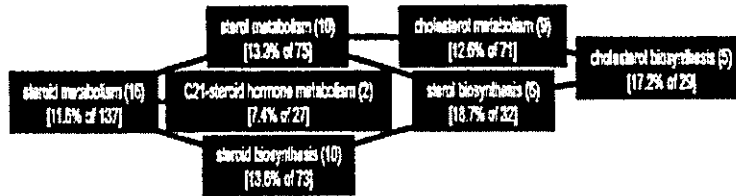
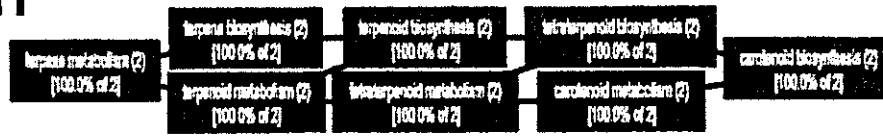


# 4OH



# Δ C2H5

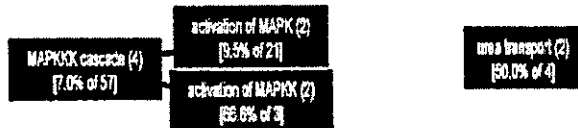
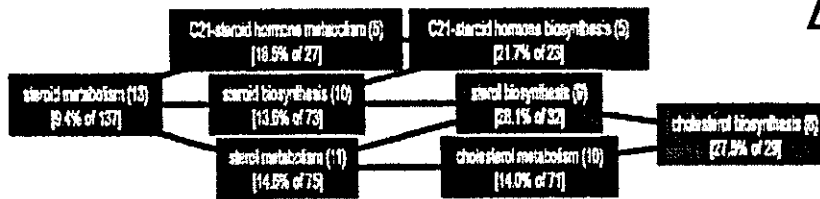




表 12 タモキシフェン誘導体処理により子宮において共通性をもって発現上昇した遺伝子

control		4OH				Tam				Tre				Δ C2Hs				Gene Name	
4h	24h	4h								24h								Gene Name	
F Raw	c F Raw	OH4hr	F Raw	TAM4h	F Raw	Tre4h	b F Raw	chem4h	F Raw	OH24h	F Raw	TAM24h	F Raw	Tre24h	F Raw	chem24h	F Raw	score	Description
A 20	N 24	4652	P 497	5034	P 914	3890	P 72	1854	P 303	144.03	P 3388	107.30	P 2716	104.69	P 2543	3.37	P 82	8	kallikrein 8
A 13	P 25	1899	P 176	2229	P 287	325	P 43	472	P 59	8.83	P 216	10.99	P 290	9.85	P 249	1.22	P 31	7	interleukin 1 receptor, type II
P 44	P 54	929	P 385	1190	P 487	228	P 99	9.85	P 392	8.72	P 295	7.10	P 394	5.26	P 280	2.64	P 141	7	MAD2 (mitotic arrest deficient, homolog)-II
A 17	A 26	9541	P 1834	126.00	P 1949	2740.0	P 461	79.63	P 1250	66.63	P 1671	29.50	P 685	29.86	P 770	20.77	A 538	7	kallikrein 8
A 1	A 1	1641	P 19	13.84	P 15	6.44	A 8	8.58	P 11	69.22	P 59	47.46	P 44	62.18	P 74	19.33	P 17	7	S100 calcium binding protein 14
P 40	P 60	426	P 161	6.01	P 223	1.32	A 52	4.37	P 163	4.91	P 279	6.27	P 387	5.49	P 325	0.94	P 56	6	desmoolin 2
P 27	P 31	610	P 127	6.71	P 165	1.47	P 39	4.41	P 159	9.03	P 266	7.79	P 247	6.87	P 261	1.09	P 33	6	desmoolin 1
P 92	P 86	891	P 765	7.15	P 603	1.82	P 146	7.05	P 600	2.83	P 235	3.95	P 344	4.36	P 373	0.89	P 76	6	GADD 45 gamma
P 38	P 73	324	P 116	8.18	P 181	1.08	P 41	3.79	P 133	3.57	P 251	2.49	P 186	3.25	P 237	0.66	P 48	6	galactose-4-epimerase, UDP
P 64	P 50	385	P 238	5.19	P 308	1.08	P 66	9.19	P 191	8.46	P 263	6.39	P 332	6.73	P 335	0.92	P 46	6	Jan domain protein 2
P 21	P 31	2348	P 483	32.23	P 623	2.74	P 57	7.65	P 147	62.00	P 1548	69.09	P 1894	42.37	P 1304	1.06	P 33	6	kallikrein 24
P 25	P 28	374	P 87	5.32	P 122	1.05	P 26	6.76	P 133	4.63	P 121	6.84	P 159	14.03	P 387	1.48	P 41	6	similar to isocitanyl-diphosphate delta-iso
P 248	P 372	3.67	P 854	8.07	P 1845	1.30	P 318	2.73	P 862	5.89	P 2107	5.97	P 2294	8.74	P 2124	0.84	P 311	6	peptidyl arginine deiminase, type II
P 158	P 269	11.85	P 1759	8.00	P 1168	1.60	P 249	7.99	P 1112	4.57	P 1134	5.73	P 1800	5.89	P 1498	0.87	P 233	6	purine-nucleoside phosphorylase
P 41	P 207	532	P 203	11.00	P 413	1.02	P 41	6.87	P 4	3.2	P 65	7.0	P 379	8.21	P 385	7.04	P 317	1	A 12
A 16	P 45	882	P 104	13.97	P 195	0.51	A 41	4.32	P 85	7.0	P 379	8.21	P 385	7.04	P 317	0.27	A 1	2	apolipoprotein B editing complex 2
A 44	P 37	858	P 463	7.17	P 233	1.62	P 71	4.85	P 200	3.96	P 140	4.56	P 174	7.00	P 256	0.55	P 20	6	adult male disincaprotein cDNA/protein
A 22	P 78	118	P 86	13.48	P 273	1.49	P 32	7.54	P 165	4.44	P 334	5.90	P 478	4.32	P 338	0.66	P 51	6	RKEN cDNA A930031D07 gene
A 42	A 58	1748	P 871	16.17	P 495	2.38	A 97	6.53	P 253	31.92	P 1789	24.86	P 1483	15.89	P 908	0.63	A 37	6	kallikrein 21
P 282	P 491	308	P 759	9.90	P 1427	1.07	P 277	3.20	P 781	3.28	P 1524	3.25	P 1657	3.90	P 1906	0.83	P 409	6	karatin complex 2, basic, gene 7
A 3	P 19	2577	P 80	51.36	P 156	1.30	A 4	20.89	P 64	4.91	P 88	7.65	P 148	12.92	P 237	0.83	P 16	6	stratifin
P 32	P 23	491	P 149	4.78	P 142	1.12	P 36	3.64	P 107	3.69	P 80	8.82	P 136	4.40	P 99	0.99	P 22	6	paired related homeobox 2
P 215	P 156	293	P 592	3.96	P 185	1.77	P 47	3.89	P 778	5.93	P 892	1.42	P 1201	7.53	P 1172	1.43	P 223	6	aldolase dehydrogenase family 1, subfamily
P 27	P 31	404	P 104	3.94	P 99	1.77	P 47	4.60	P 114	3.32	P 98	2.13	P 88	5.91	P 119	1.73	P 53	5	RKEN cDNA 2810307C23 gene
P 22	P 30	348	P 70	4.76	P 95	1.24	P 26	3.74	P 75	2.38	P 69	3.85	P 114	7.34	P 220	1.07	P 32	5	cytochrome P450, 51
P 86	P 91	172	P 138	3.93	P 288	0.99	P 84	3.62	P 289	2.76	P 241	6.70	P 536	5.79	P 621	2.15	P 185	5	farnesyl diphosphate synthetase
P 118	P 81	217	P 241	1.40	P 208	1.24	P 144	2.95	P 325	4.23	P 331	3.52	P 296	3.82	P 308	2.79	P 226	5	karyopherin (importin) alpha 2
P 53	P 78	356	P 197	6.08	P 248	1.30	P 68	4.88	P 231	2.36	P 178	3.01	P 317	4.63	P 360	1.01	P 79	5	low density lipoprotein receptor
P 430	P 704	8.83	P 2352	6.85	P 2394	1.39	P 388	5.38	P 2151	3.96	P 2488	2.61	P 1835	2.55	P 1788	0.92	P 649	5	purine-nucleoside phosphorylase
P 22	P 46	977	P 200	3.89	P 74	3.18	P 68	8.78	P 138	3.85	P 162	0.40	P 19	0.54	P 25	1.04	P 48	5	ribosomal protein L37a
P 21	P 44	400	P 77	8.41	P 102	1.11	P 22	5.30	P 101	1.82	P 69	2.71	P 124	8.81	P 389	0.85	P 29	5	sterol-C4-methyl oxidase-like
P 202	P 223	541	P 1025	3.34	P 820	2.01	P 399	4.66	P 875	0.75	P 160	2.99	P 578	2.70	P 599	1.10	P 245	5	splicing factor, arginine/serine-rich 2
P 28	P 28	362	P 96	3.32	P 86	0.95	P 26	4.47	P 117	3.58	P 95	2.51	P 73	3.20	P 89	2.06	P 57	5	splicing factor, arginine/serine-rich 2
P 236	P 311	287	P 637	3.82	P 832	1.02	P 236	3.00	P 859	2.69	P 775	2.33	P 750	3.24	P 902	0.81	P 251	5	taste expressed gene 2
P 114	P 156	443	P 673	6.63	P 686	1.29	P 144	2.97	P 314	8.90	P 397	2.33	P 378	2.91	P 450	0.94	P 148	5	neurturin
P 32	P 37	333	P 100	3.43	P 101	1.20	P 38	2.41	P 109	3.22	P 123	8.72	P 208	6.19	P 141	2.89	P 37	5	Nedd4 WW binding protein 4
P 59	P 23	385	P 202	4.21	P 229	1.30	P 48	3.71	P 120	6.99	P 129	8.72	P 208	6.19	P 141	2.89	P 61	5	crystallin, alpha B
P 61	P 61	146	P 83	5.03	P 336	0.81	P 46	1.55	P 17	12.65	P 37	9.05	P 69	9.28	P 76	5.67	P 45	7	41
A 10	A 22	1000	M 4	0.80	A 1	1.55	A 14	3.48	P 111	2.09	P 111	2.09	P 64	2.94	P 87	3.00	P 65	0.37	A 8
A 13	A 8	1849	P 226	13.12	P 157	1.94	A 25	14.35	P 173	2.53	A 19	20.75	P 168	19.45	P 151	0.44	A 3	5	TNF receptor superfamily, member 12a
P 24	P 45	851	P 222	12.78	P 187	2.24	P 54	7.35	P 171	2.72	P 118	4.65	P 217	4.87	P 218	0.89	P 40	5	Nedd4 WW binding protein 4
P 536	P 585	2.99	P 1505	3.60	P 1728	1.18	P 624	3.03	P 1510	2.11	P 1150	2.96	P 1734	3.81	P 2030	1.16	P 655	5	receptor (calcitonin) activity modifying prot
P 116	A 130	3.23	P 687	6.80	P 383	1.10	M 125	8.37	P 899	1.31	P 183	3.79	P 375	3.46	P 446	1.10	P 142	5	serum-inducible phospho
P 41	P 58	4.73	P 184	5.36	P 205	1.40	P 57	4.41	P 170	2.27	P 123	3.84	P 189	3.08	P 173	1.03	P 58	5	melanophin
A 24	P 27	3.91	P 80	3.29	P 74	1.83	A 4	3.23	P 73	2.80	P 74	3.78	P 108	3.33	P 91	0.92	A 25	6	ret proto-oncogene
P 67	P 68	7.15	P 450	5.56	P 282	2.16	P 143	4.62	P 350	1.91	P 126	3.35	P 237	3.71	P 252	1.20	P 82	5	chemokine orphan receptor 1
P 13	A 12	8.84	P 67	6.58	P 66	1.22	A 15	5.19	P 82	3.76	A 43	3.81	P 47	5.35	P 63	0.87	A 10	5	histamine receptor H 1
A 22	P 21	7.07	P 148	7.08	P 146	2.25	P 49	10.65	P 221	3.74	P 55	5.93	P 128	4.81	P 93	1.03	A 22	5	a disintegrin-like and metalloprotease
P 21	P 19	8.89	P 127	4.83	P 94	1.14	P 24	4.40	P 88	3.22	M 60	6.90	P 134	7.48	P 139	1.02	A 19	5	parathyroid hormone-like peptide
P 8	P 8	9.00	P 62	7.02	P 54	1.78	P 15	4.12	P 32	6.03	M 47	6.47	P 54	6.42	P 43	0.86	P 7	5	parathyroid hormone-like peptide
A 22	A 7	13.83	P 286	19.45	P 212	0.58	A 12	12.63	P 256	9.11	A 61	30.14	P 218	31.93	P 219	0.93	A 6	5	TNF receptor superfamily, member 12a

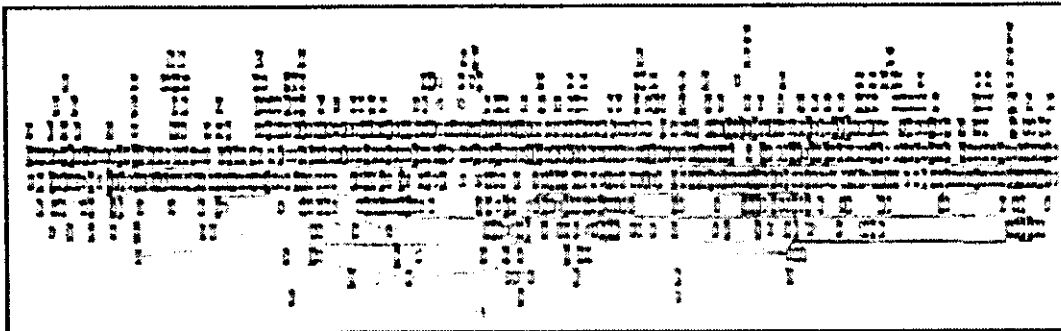
表 13 タモキシフェン誘導体処理により子宮において共通性をもって発現低下した遺伝子

control		4OH				Tam				Tre				Δ C2Hs				Gene Name	
4h	24h	4h								24h								Gene Name	
F Raw	c F Raw	OH4hr	F Raw	TAM4h	F Raw	Tre4h	b F Raw	chem4h	F Raw	OH24h	F Raw	TAM24h	F Raw	Tre24h	F Raw	chem24h	F Raw	score	Description
P 173	P 491	0.23	P 37	0.14	P 23	0.84	P 159	0.35	P 57	0.30	A 26	0.21	P 20	0.18	P 15	1.20	P 109	6	N-auriferase
P 350	P 489	0.26	P 114	0.31	P 101	0.83	P 321	0.24	P 79	0.24	P 112	0.56	P 192	0.24	P 118	1.26	P 615	6	D site albumin promoter binding protein
P 534	P 328	0.32	P 180	0.29	P 142	0.72	P 378	0.39	P 195	0.41	P 128	0.37	P 126	0.31	P 101	0.94	P 306	6	glucocorticoid-induced leucine zipper
P 196	P 83	0.40	P 70	0.19	A 33	0.87	P 159	0.36	A 82	0.13	A 12	0.25	A 24	0.09	A 8	1.15	P 106	6	flavin containing monooxygenase 2
P 820	P 781	0.26	P 190	0.84	P 182	0.98	P 791	0.37	P 284	0.32	P 240	0.23	P 183	0.28	P 204	1.14	P 891	6	REV3-like
P 49	P 37	0.36	P 16	0.38	P 12	1.24	P 59	0.26	P 13	0.03	A 1	0.09							

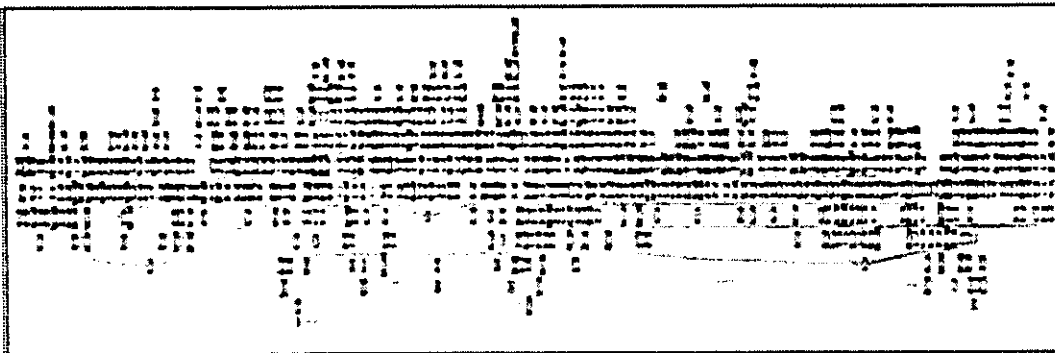
表14 タモキシフェン誘導体処理したマウス子宮でのエストロゲンレセプター関連遺伝子群の発現変化

4OH			Tam			Tres			AC2H5			Common	Gene	Description											
4hr	F/Raw	24hr	F/Raw	24hr	F/Raw	4hr	F/Raw	24hr	F/Raw	4hr	F/Raw				24hr	F/Raw									
0.33	P	118	0.71	P	351	0.73	P	251	0.80	P	317	0.85	P	317	0.78	P	390	0.51	P	179	0.63	P	354	Trim25	tripartite motif protein 25(elf)
2.20	P	1939	0.87	P	4498	2.77	P	2990	0.47	P	2614	0.89	P	916	0.30	P	1599	0.97	P	847	0.33	P	1697	Lif	leukemia inhibitory factor
1.84	P	578.4	1.95	P	594.4	1.45	P	502.4	0.8	P	280.7	1.34	P	494.2	0.72	P	228.2	1.74	P	607.9	1.04	P	328.7	TFF1	trifolion factor 1(breast cancer estrogen-inducible sequ keratin19)
1.18	P	854.7	2.24	P	2424	2.17	P	1591	1.8	P	2128	0.9	P	702	2.08	P	2337	1.44	P	1067	1.14	P	1278	NRT1-	hepatocyte growth factor
0.41	A	7	0.71	A	15	0.43	A	7	0.57	P	13	1.19	A	21	0.28	A	6	0.57	A	10	0.85	P	19	Hgf	Mus sp. mRNA for oxytocin receptor, complete cds.
3.02	P	62	3.67	P	87	2.00	A	40	2.34	P	46	1.19	A	25	1.41	M	27	2.71	A	55	1.30	A	25	Oxtr	complement component 3
1.21	P	1590	1.39	P	6788	3.15	P	4100	0.68	P	3567	0.96	P	1332	0.50	P	2543	1.29	P	1692	0.40	P	2028	C3	lipocalin 2
3.28	P	1870	2.45	P	1327	7.88	P	4427	0.76	P	4442	1.00	P	602	0.70	P	3889	3.54	P	2004	0.40	P	1367	Len2	cathepsin D
0.36	P	788	0.85	P	867	0.46	P	994	0.88	P	835	1.00	P	2335	0.78	P	894	0.78	P	1715	0.81	P	862	Cted	vascular endothelial growth factor B
0.36	A	49	0.79	A	53	0.43	A	37	0.84	M	61	1.11	M	102	0.44	A	31	0.40	A	35	1.13	P	79	Vegfb	vascular endothelial growth factor C
0.07	A	2	0.39	A	8	0.01	A	6	0.58	A	12	0.88	A	26	0.70	P	15	0.31	A	9	1.36	P	29	Vegfc	transforming growth factor, alpha
2.7	P	83.9	0.87	P	45.7	1.73	P	52.8	0.9	P	49.7	1.49	P	48.8	1	P	54.1	1.5	P	46	1.02	P	55.2	Tgfb	transforming growth factor, beta 3
0.81	P	94	0.30	A	34	0.88	P	77	0.52	P	63	0.60	P	73	0.28	P	44	0.53	P	81	1.41	P	185	Tgfb3	3-hydroxy-3-methylglutaryl-Coenzyme A reductase
2.00	P	32	0.34	A	11	2.58	P	41	1.28	P	22	1.17	P	20	3.04	P	50	2.87	P	46	0.98	P	18	Hmcr	progesterone receptor
2.19	P	107.1	2.04	P	58.2	1.81	P	77.1	2.3	P	72.2	1.07	P	54.8	1.34	P	40	1.68	P	61.3	1.53	P	46.1	PQR	estrogen receptor 1 (alpha)
2.30	P	47	0.83	A	35	0.01	A	7	1.07	P	50	2.40	A	54	0.26	A	11	1.04	A	22	1.13	P	51	Ear1	estrogen receptor-binding site-associated antigen 9
0.85	P	110.6	0.95	P	110.5	0.7	P	90.3	1	P	129.7	1	P	136.1	1.13	P	135.7	0.74	P	95.3	0.88	P	118.7	ERAS3	insulin-like growth factor binding protein 4
0.57	P	188	0.68	A	160	0.45	M	159	1.07	P	271	0.81	P	312	0.55	P	134	0.55	P	177	1.58	P	385	Igfbp4	insulin-like growth factor 1
1.10	P	310	4.51	P	582	1.39	P	384	3.82	P	753	1.08	P	321	3.69	P	491	2.14	P	599	1.95	P	261	Igf1	insulin-like growth factor 1 receptor
1.16	P	184	3.16	P	220	1.14	P	204	3.26	P	391	1.06	P	188	3.13	P	223	2.25	P	372	2.49	P	178	Igf1r	E2F transcription factor 1
0.90	A	63	0.88	A	50	0.01	P	45	0.46	P	66	1.02	P	135	0.23	P	32	0.43	P	53	0.76	P	105	Igf1r1	E2F transcription factor 1
2.16	A	30	0.21	P	75	1.03	A	14	2.13	P	33	0.39	A	6	2.75	P	41	1.52	A	21	1.02	P	15	E2f1	low density lipoprotein receptor
3.88	P	197	2.36	P	178	5.08	P	248	3.91	P	317	1.30	P	68	4.83	P	380	4.88	P	231	1.01	P	79	Ldlr	low density lipoprotein receptor
3.96	P	197	2.36	P	178	5.08	P	248	3.91	P	317	1.30	P	68	4.83	P	380	4.88	P	231	1.01	P	79	Ldlr	FBJ osteosarcoma oncogene
5.41	P	443	1.01	P	276	3.19	P	417	0.89	P	262	1.42	P	121	1.25	P	354	6.08	P	492	0.43	P	122	Fox	B-cell leukemia/lymphoma 2
0.88	A	88	0.67	A	33	0.58	A	42	0.93	P	49	0.92	P	315.9	2.13	P	575	1.91	P	578	1.06	P	287.8	lend1	end1
1.84	P	584.4	1.82	P	476.5	1.75	P	526.6	1.7	P	480	0.89	P	236.3	2.01	P	287.5	2.24	P	338	0.92	P	122.4	pcnd1	pcnd1
1.84	P	584.4	1.82	P	476.5	1.75	P	526.6	1.7	P	480	0.89	P	236.3	2.01	P	287.5	2.24	P	338	0.92	P	122.4	pcnd1	pcnd1
1.29	P	60.3	1.3	A	52.1	1.79	P	82.2	1.6	P	70.5	1.17	P	87.4	2.01	P	83.4	1.81	P	84.1	0.93	P	38.6	pcnd1	pcnd1
1.43	P	317.8	1.74	P	344	1.18	P	257.3	1.7	P	360.9	1.1	P	254.4	1.39	P	283.4	1.44	P	315.8	1.04	P	212.1	pcnd3	pcnd3
0.44	P	17	1.48	A	32	0.88	P	33	3.86	P	91	0.93	P	37	3.76	P	83	1.00	P	38	2.42	P	53	Serpinc1a	ovalbumin
1.8	P	10.8	0.38	A	2.8	1.53	P	9	0.4	A	3	1.34	P	8.4	0.22	A	1.5	1.33	A	7.9	0.41	A	2.8	Bcl2	breast cancer 1
0.90	M	14	4.24	P	40	0.83	A	12	3.84	P	41	1.39	P	22	6.18	P	50	1.83	P	28	2.77	P	27	Bcl1	myelocytomatosis oncogene
0.59	P	136	0.45	A	79	0.43	P	99	0.54	P	102	1.02	P	247	0.27	P	64	0.79	P	182	0.76	P	138	Mye	creatine kinase, mitochondrial 1, ubiquitous
1.57	P	78	1.74	P	273	5.84	P	257	1.73	P	292	1.43	P	75	2.28	P	370	2.70	P	134	0.86	P	139	Ckmt1	eNOS
1.82	P	121.8	1.89	P	87.8	1.5	P	98.9	1.7	P	72.8	0.8	P	66.1	1.37	P	56.8	1.27	P	84.2	0.85	P	39.5	NO3	matrix metalloproteinase 11
0.83	P	44	0.30	P	172	0.48	P	25	0.36	P	144	1.11	P	62	0.33	P	128	0.52	P	27	0.87	P	280	Mmp11	matrix metalloproteinase 14 (membrane-inserted)
0.80	P	101	0.37	P	57	0.68	P	76	0.93	P	153	0.89	P	107	0.48	P	74	0.79	P	90	0.94	P	149	Mmp14	matrix metalloproteinase 15
0.60	A	17	1.78	A	31	0.26	A	7	3.16	P	59	0.76	A	22	7.74	P	84	0.15	A	4	1.28	P	23	Mmp15	matrix metalloproteinase 17
1.56	P	87	3.81	P	134	1.91	P	88	1.59	P	63	1.43	P	84	1.33	P	51	1.54	P	65	1.12	P	43	Mmp17	matrix metalloproteinase 19
2.91	M	74	3.90	A	60	0.79	P	20	2.83	P	48	1.31	M	35	1.91	P	30	1.51	P	38	2.33	P	37	Mmp19	matrix metalloproteinase 3
0.72	A	19	0.16	A	7	1.01	A	26	0.18	A	9	0.80	A	24	0.11	A	5	0.83	A	21	0.50	A	23	Mmp3	matrix metalloproteinase 7
4.21	P	198	1.04	A	184	2.77	A	127	0.68	P	133	0.89	A	43	0.80	P	154	1.30	A	60	0.23	A	45	Mmp7	CEA-related cell adhesion molecule 1
0.69	A	33	0.34	A	153	3.84	P	152	0.72	P	321	0.99	A	50	0.27	P	147	1.92	P	91	0.40	P	121	Cacacm1	CEA-related cell adhesion molecule 1
1.12	P	37	0.34	A	37	1.62	P	59	0.45	P	63	1.35	A	47	0.27	P	29	2.37	A	78	0.40	P	42	Cacacm1	CEA-related cell adhesion molecule 2
1.08	P	289	0.69	P	820	2.36	P	574	0.68	P	854	1.02	P	284	0.53	P	651	1.50	P	368	0.40	P	366	Cacacm2	CEA-related cell adhesion molecule 2
0.91	P	157	0.63	P	541	2.21	P	376	0.56	P	523	0.87	P	157	0.44	P	368	1.46	P	251	0.40	P	278	Cacacm2	flavin cont flavin-containing monooxygenase 2
0.40	A	70	0.34	A	12	1.18	A	33	0.25	A	24	0.87	P	159	0.27	A	8	0.38	A	62	1.18	P	106	Fmo2	flavin cont flavin-containing monooxygenase 2
0.43	A	63	0.41	A	27	0.28	M	34	0.24	M	17	0.78	P	100	0.27	A	2	0.17	A	21	0.73	P	50	Fmo2	interleukin 6 signal transducer
0.93	P	116	0.24	A	25	0.59	P	72	0.74	P	110	0.69	P	90	0.27	A	15	0.56	P	69	1.38	P	197	Stat	Tnf-related adipose-related protein
0.55	A	44	1.00	A	134	0.33	P	42	0.51	P	74	1.57	P	102	0.27	A	32	0.65	M	52	0.40	P	48	Tnfr-pendin	tumor necrosis factor, alpha-induced protein 2
2.43	P	40	0.34	A	19	2.05	P	33	0.48	P	33	1.09	P	19	0.42	P	27	2.17	P	38	0.40	P	15	Tnfrap2	tumor necrosis factor receptor superfamily, member 1
0.95	A	3	0.34	A	0	0.12	A	0	0.85	A	3	1.40	P	5	0.45	A	2	1.37	A	5	1.18	M	4	Tnfr11b	tumor necrosis factor receptor superfamily, member 1
0.15	A	5	0.28	A																					

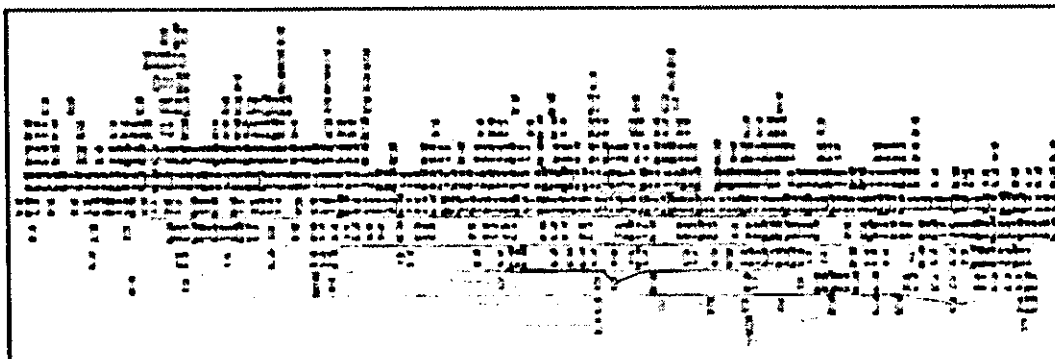
図6 タモキシフェン誘導体処理した子宮において選択した遺伝子の Ontology tree 解析



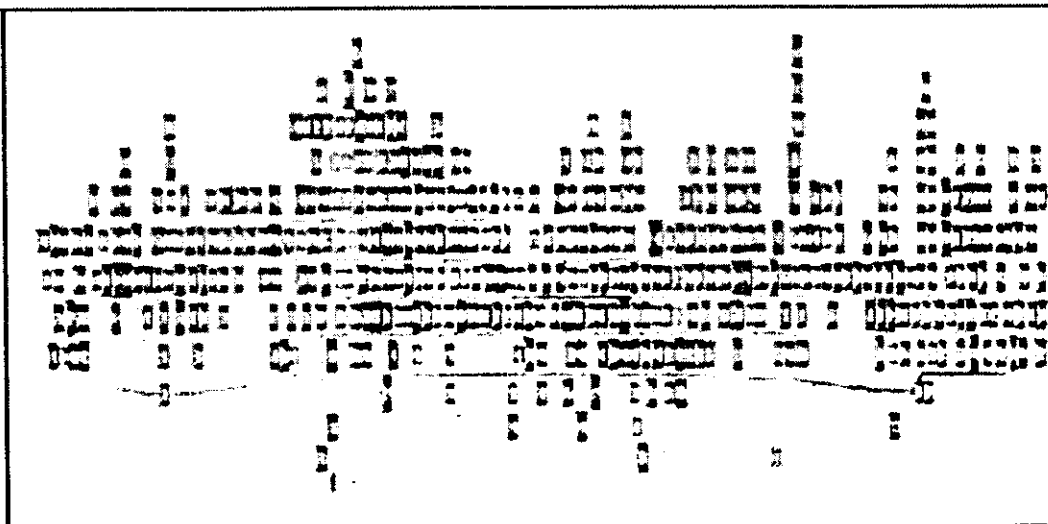
Tre



4OH



Tam



ΔC2H5

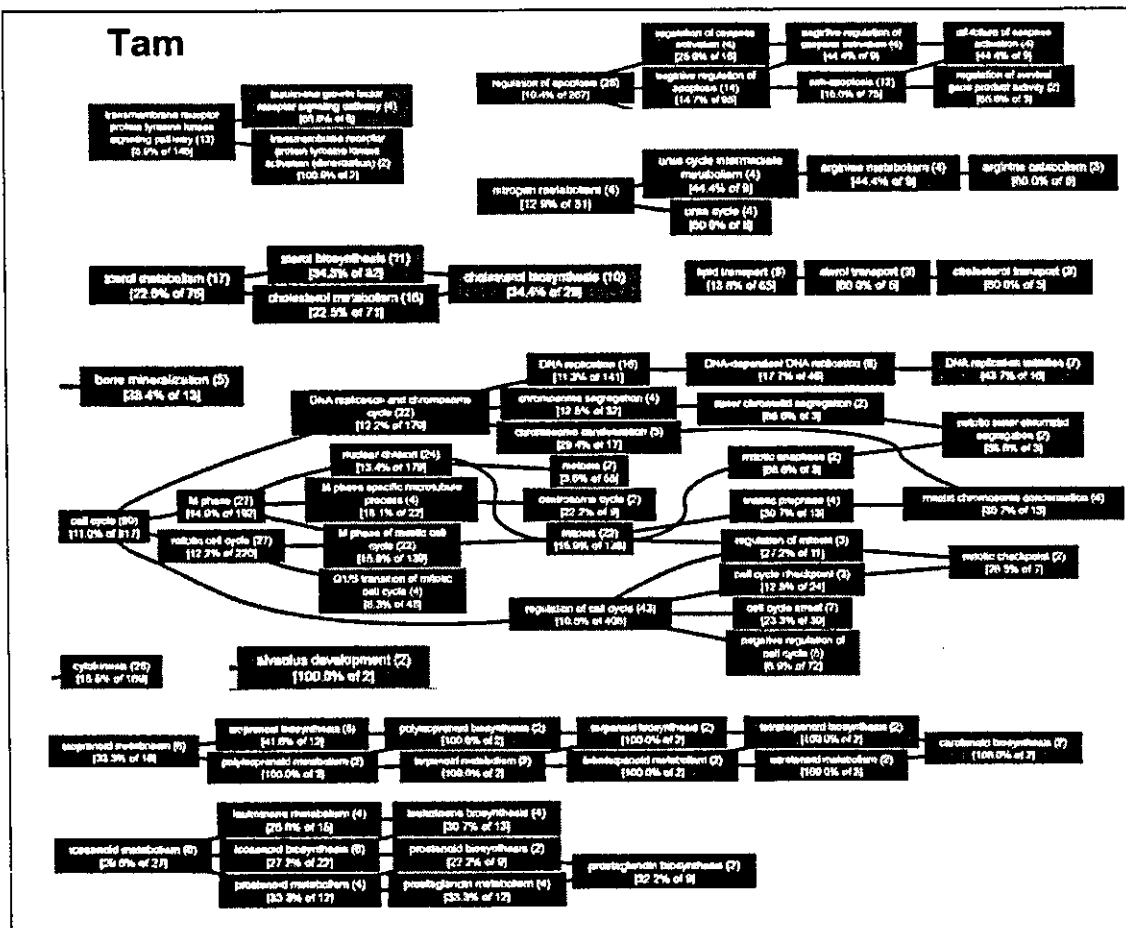
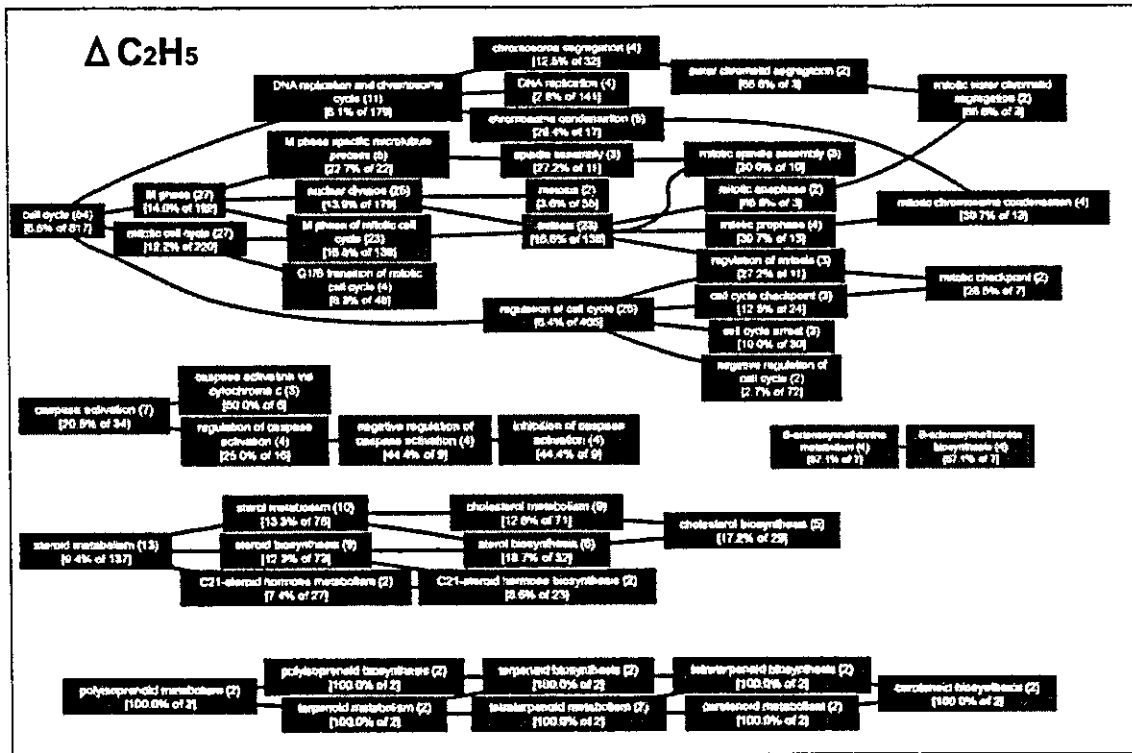




図7 遺伝子発現データベースの構造

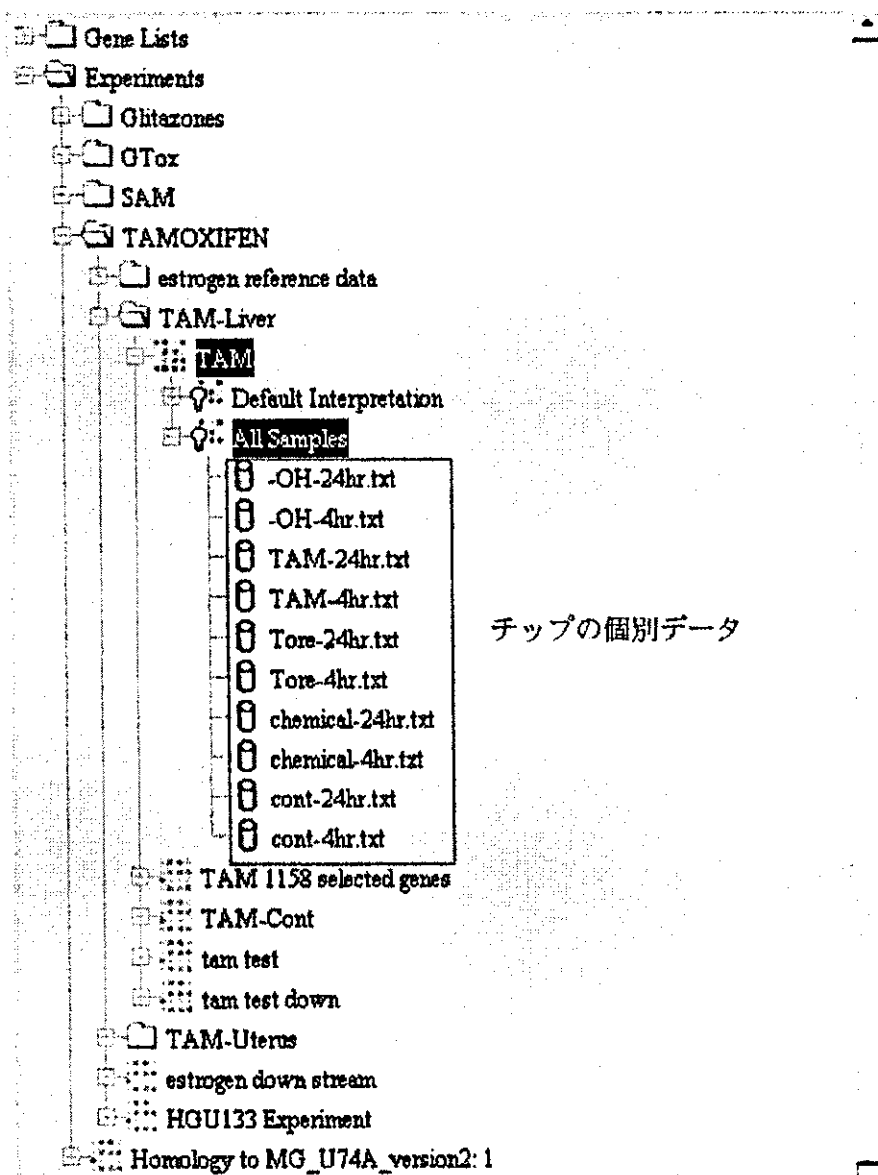


図 8 ヒトデータとマウスデータの直接比較法 (HU133A から MOE430 への変換の例)

1. Excel にて HU133A MOE430 アレイのプローブ ID をリストアップした表を作成。

	A	B
1	221517_s_ε1451719_at	
2	209708_at	1422643_at
3	221407_at	1423019_at
4	214886_s_ε1417707_at	
5	204843_s_ε1452915_at	
6	202780_at	1428140_at

2. このファイルを MOE430.homology という名前で、GeneSpring の HU133 チップフォルダー内にある "Homology Tables" というフォルダへ保存する。

3. これにより、自動的に HU133A チップでの遺伝子リストをマウスのゲノムへ変換するための準備が整うが、GeneSpring 上で変換操作を行うと、両者のデータは横並びには表示されず、対応するマウスのチップ上のプローブ ID のみが右のように表示される。

Summary for 133A

Total number of genes: 22,921

1: Systemat	2: Common Na	23: mouse homolog	27: A
224	202077_at	1428160_at	
224	202078_at	1416678_at	
224	202079_at KIAA1042		
224	202080_at	1428327_at	
224	202081_at	1416442_at	
224	202082_at	1451002_at	

OK Cancel Help

4. 次に mouse homolog ID を含む HU133A データを表形式で Excel 上へ書き出すと右の表の左側の赤色で示した部分に mouse homolog (青色) が追加される。

	A	B	C	D	E	F	G	H	I	J	K	L	M	N	O	P	Q	R	S	T	U	V	W	X	Y	Z
1	Systemat	TAM133A	TAM133A	TAM133A	Gene	mouse homolog																				
2	202077_at	106 P	567 004 P	410	126 F	821 NM_001537	1428160_at	1428160	112	132 P	132	006 P	80													
3	202078_at	092 P	325 001 F	270	095 P	420 NM_002810	1422643_at	1424136	79	093 P	57	147 P	85													
4	202079_at	111 P	32 089 P	30	040 F	29 NM_016409	1416678_at	1416678	120	115 P	152	116 P	124													
5	202080_at	092 P	258 015 P	252	070 F	269 NM_001833	1416442_at	1416442	209	116 P	150	003 P	102													
6	202081_at	076 F	47 057 P	107	054 F	62 NM_037107	1415730_at	1415730	145	106 P	787	102 P	910													
7	202082_at	140 F	523 111 P	705	084 F	568 NM_003820	1452915_at	1448114	1000	104 P	1110	106 P	841													
8	202083_at	071 P	71 052 P	46	116 F	90 BC009654	1451312_at	1451312	154	116 P	859	114 P	745													
9	202084_at	128 P	125 063 P	117	081 P	121 NM_001379	1428176_at	1428176	111	081 P	121	081 P	112													
10	202085_at	100 F	336 023 P	240	095 F	132 NM_014395	1416642_at	1416642	117	081 P	121	081 P	112													
11	202086_at	089 P	49 143 P	107	144 F	61 BC020218	1415764_at	1415764	223	057 P	194	114 P	243													
12	202087_at	101 P	590 023 P	494	175 F	803 NM_004251	1428327_at	1428327	142	110 A	141	110 P	101													
13	202088_at	060 F	89 155 P	176	153 F	94 BC009650	1452915_at	1448038	60	113 P	75	091 P	81													
14	202089_at	104 P	252 197 P	450	162 F	200 NM_014165	1427927_at	1427927	111	101 P	270	130 P	163													
15	202090_at	141 P	191 142 P	252	103 F	150 NM_018261	1453217_at	1453217	145	106 P	110	106 P	101													
16	202091_at	106 F	83 072 P	70	052 P	58 NM_018647	1448542_at	1448542	406	100 P	306	122 P	407													
17	202092_at	136 P	98 131 P	125	125 F	71 NM_018101	1448450_at	1448450	142	110 A	114	044 A	5													
18	202093_at	096 A	5 041 A	4	843 M	9 NM_001298	1429496_at	1429496	142	110 A	114	044 A	5													
19	202094_at	164 P	104 146 P	75	131 P	84 NM_001304	1417322_at	1417322	50	111 P	96	080 P	76													
20	202095_at	141 P	165 061 P	105	107 F	110 NM_003206	1416655_at	1416655	38	090 A	23	150 P	21													
21	202096_at	066 P	190 120 P	180	092 P	85 NM_014060	1448019_at	1448019	1448	106 P	1100	122 P	1688													
22	202097_at	138 P	84 141 P	132	080 P	141 NM_003240	1429567_at	1429567	1420	021 P	154	106 P	132													
23	202098_at	102 P	96 058 A	71	043 F	41 BC029550	1429474_at	1429474	100	114 P	146	107 P	120													
24	202099_at	146 P	62 042 P	27	086 F	40 BC008201	1451144_at	1451144	145	095 P	100	114 P	146													
25	202100_at	134 P	76 076 P	207	076 P	217 BC149336	1429759_at	1429759	1426	100 P	111	121 P	409													
26	202101_at	128 P	290 115 P	216	039 P	152 AF151842	1428252_at	1428252	152	039 P	152	039 P	152													

5. 次に、この mouse homolog を用いて MOE430 用の遺伝子リストを作成し、GeneSpring 上で対応するマウスチップのデータから対応するデータをリストアップし、同様に Excel 上へ転送する。

6. Mouse homolog の項をキーとして HU133A および MOE430 のデータを並び替え、一部重複する項目を手作業にて整理することにより両者を一つの Excel ファイル上で横並びの表として結合させる。これにより、両者のデータを用いてスクアープロットを書かせるなどの直接比較が可能となる。

	A	B	C	D	E	F	G	H	I	J	K	L	M	N	O	P	Q	R	S	T	U	V	W	X	Y	Z
1	Systemat	TAM133A	TAM133A	TAM133A	Gene	mouse homolog																				
2	202077_at	106 P	567 004 P	410	126 F	821 NM_001537	1428160_at	1428160	112	132 P	132	006 P	80													
3	202078_at	092 P	325 001 F	270	095 P	420 NM_002810	1422643_at	1424136	79	093 P	57	147 P	85													
4	202079_at	111 P	32 089 P	30	040 F	29 NM_016409	1416678_at	1416678	120	115 P	152	116 P	124													
5	202080_at	092 P	258 015 P	252	070 F	269 NM_001833	1416442_at	1416442	209	116 P	150	003 P	102													
6	202081_at	076 F	47 057 P	107	054 F	62 NM_037107	1415730_at	1415730	145	106 P	787	102 P	910													
7	202082_at	140 F	523 111 P	705	084 F	568 NM_003820	1452915_at	1448114	1000	104 P	1110	106 P	841													
8	202083_at	071 P	71 052 P	46	116 F	90 BC009654	1451312_at	1451312	154	116 P	859	114 P	745													
9	202084_at	128 P	125 063 P	117	081 P	121 NM_001379	1428176_at	1428176	111	081 P	121	081 P	112													
10	202085_at	100 F	336 023 P	240	095 F	132 NM_014395	1416642_at	1416642	117	081 P	121	081 P	112													
11	202086_at	089 P	49 143 P	107	144 F	61 BC020218	1415764_at	1415764	223	057 P	194	114 P	243													
12	202087_at	101 P	590 023 P	494	175 F	803 NM_004251	1428327_at	1428327	142	110 A	141	110 P	101													
13	202088_at	060 F	89 155 P	176	153 F	94 BC009650	1452915_at	1448038	60	113 P	75	091 P	81													
14	202089_at	104 P	252 197 P	450	162 F	200 NM_014165	1427927_at	1427927	111	101 P	270	130 P	163													
15	202090_at	141 P	191 142 P	252	103 F	150 NM_018261	1453217_at	1453217	145	106 P	110	106 P	101													
16	202091_at	106 F	83 072 P	70	052 P	58 NM_018647	1448542_at	1448542	406	100 P	306	122 P	407													
17	202092_at	136 P	98 131 P	125	125 F	71 NM_018101	1448450_at	1448450	142	110 A	114	044 A	5													
18	202093_at	096 A	5 041 A	4	843 M	9 NM_001298	1429496_at	1429496	142	110 A	114	044 A	5													
19	202094_at	164 P	104 146 P	75	131 P	84 NM_001304	1417322_at	1417322	50	111 P	96	080 P	76													
20	202095_at	141 P	165 061 P	105	107 F	110 NM_003206	1416655_at	1416655	38	090 A	23	150 P	21													
21	202096_at	066 P	190 120 P	180	092 P	85 NM_014060	1448019_at	1448019	1448	106 P	1100	122 P	1688													
22	202097_at	138 P	84 141 P	132	080 P	141 NM_003240	1429567_at	1429567	1420	021 P	154															



表 17 グリタゾン化合物各処理間でのデータの相関性の比較

Pioglitazone		Rosiglitazone		Troglitazone	
処理	相関係数	処理	相関係数	処理	相関係数
1P20,1P200	0.87	1R20,1R200	0.91	1T20,1T200	0.85
24P20,24P200	0.52	72R20,72R200	0.53	4T20,4T200	0.45
1P20,4P20	0.41	1R20,4R20	0.47	1T20,4T20	0.38
1P200,4P20	0.39	4R20,4R200	0.45	24T20,24T200	0.36
4P20,72P20	0.37	1R200,4R20	0.39	72T20,72T200	0.28
1P20,24P20	0.31	4R20,72R20	0.32	4T20,72T20	0.26
24P20,72P20	0.30	4R20,72R200	0.30	1T200,4T20	0.18
1P20,72P20	0.29	24R20,72R20	0.29	24T,72T	0.16
1P200,24P200	0.23	24R20,24R200	0.26	1T20,4T200	0.14
72P20,72P200	0.23	1R20,72R200	0.22	4T,72T	0.13
1P20,24P200	0.22	1R200,72R200	0.19	4T20,24T20	0.12
4P20,24P20	0.21	4R200,72R200	0.15	1T,4T	0.12
4P200,72P200	0.19	4R20,24R20	0.15	24T20,72T200	0.11
1P200,24P20	0.19	1R20,72R20	0.15	24T20,72T20	0.10
1P200,72P20	0.17	4R200,72R20	0.09	1T20,24T200	0.10
4P20,24P200	0.13	1R200,72R20	0.08	24T200,72T20	0.09
4P20,4P200	0.12	1R20,24R	0.08	1T200,24T200	0.09
1P,24P	0.12	72R200,24R	0.07	1T20,72T20	0.09
24P200,72P20	0.10	4R200,24R	0.07	24T200,72T200	0.06
1P,72P	0.09	1R20,24R20	0.07	4T200,72T20	0.06
4P,24P	0.09	4R20,24R	0.06	1T200,4T200	0.06
72P20,24P	0.08	4R,72R	0.06	1T20,72T	0.06
72P200,1P	0.06	1R,72R	0.06	1T200,72T	0.05
4P,72P	0.05	72R20,24R	0.06	1T200,1T	0.05
1P,4P	0.05	1R200,24R	0.05	4T,24T	0.05
24P20,1P	0.05	1R20,4R200	0.05	1T,72T	0.04
1P200,24P	0.05	24R200,1R	0.05	24T200,72T	0.04
72P200,4P	0.05	24R,72R	0.05	24T200,4T	0.04
24P20,24P	0.04	4R200,24R200	0.04	72T20,24T	0.04
1P20,24P	0.04	1R200,72R	0.04	72T200,24T	0.03
4P20,24P	0.04	4R200,24R20	0.03	4T200,24T200	0.03
72P20,4P	0.03	1R20,72R	0.03	1T200,4T	0.03
4P200,4P	0.02	24R200,4R	0.03	24T20,4T	0.02
72P200,24P	0.02	4R200,4R	0.03	72T200,4T	0.01
72P20,72P	0.02	24R20,1R	0.02	1T20,1T	0.01
72P20,1P	0.02	24R20,72R200	0.02	4T20,72T	0.01
1P20,72P	0.01	1R200,4R200	0.02	24T200,24T	0.01
1P20,1P	0.01	72R20,1R	0.02	1T20,4T	0.01
1P200,72P	0.01	1R,24R	0.02	4T200,72T	0.01
72P200,72P	0.01	1R200,24R20	0.01	24T200,1T	0.01
24P,72P	0.01	24R20,4R	0.01		

	time point (hr)	dose
in vivo	1,4,24,72	20 mg/kg, 200 mg/kg
in vitro	1,4,24,72	30 uM

別添5

III. 研究成果の刊行に関する一覧表  
平成16年度

## 研究成果の刊行に関する一覧表(平成16年度)

雑誌

	発表者氏名	論文タイトル名	発表誌名	巻号	ページ	出版年
1)	Takayoshi Suzuki, Yuki Nagano, Akiyasu Kouketsu, Azusa Matsuura, Sakiko Maruyama, Mineko Kurotaki, Hidehiko Nakagawa, <u>Naoki Miyata</u>	Novel inhibitors of human histone deacetylases: design, synthesis, enzyme inhibition, and cancer cell growth inhibition of SAHA-based non-hydroxamates	<i>J. Med. Chem.</i>	48	1019-1032	2005
2)	Shinya Usui, Takayoshi Suzuki, Yoshifumi Hattori, Kazuma Etoh, Hiroki Fujieda, Makoto Nishizuka, Masayoshi Imagawa, Hidehiko Nakagawa, Kohfuku Kohda, <u>Naoki Miyata</u>	Design, synthesis and biological activity of novel PPAR $\gamma$ ligands based on rosiglitazone and 15d-PGJ2	<i>Bioorganic &amp; Medicinal Chemistry Letters</i>	15	1547-1551	2005
3)	Takayoshi Suzuki, Azusa Matsuura, Akiyoshi Kouketsu, Hidehiko Nakagawa, <u>Naoki Miyata</u>	Identification of a potent non-hydroxamate histone deacetylase inhibitor by mechanism-based drug design	<i>Bioorganic &amp; Medicinal Chemistry Letters</i>	15	331-335	2005
4)	Takayoshi Suzuki, Akiyasu Kouketsu, Azusa Matsuura, Arihiro Kohara, <u>Shin-ichi Ninomiya</u> , Kohfuku Kohda, <u>Naoki Miyata</u>	Thiol-based SAHA analogues as potent histone deacetylase inhibitors,	<i>Bioorganic &amp; Medicinal Chemistry Letters</i>	14(12)	3313-3317	2004
5)	Masaaki Kurihara, Abu Shara Shamsur Rouf, Hisao Kansui, Hiroyuki Kagechika, <u>Haruhiro Okuda</u> , <u>Naoki Miyata</u>	Design and synthesis of cyclic urea compounds: a pharmacological study for retinoidal acty	<i>Bioorganic &amp; Medicinal Chemistry Letters</i>	14(16)	4131-4134	2004
6)	Eiji Okada, Yuka Komazawa, Masaaki Kurihara, Hideshi Inoue, <u>Naoki Miyata</u> , <u>Haruhiro Okuda</u> , Toshie Tsuchiya, Yoko Yamakoshi	Synthesis of C60 derivatives for photoaffinity labeling	<i>Tetrahedron Letters</i>	45(3)	527-529	2004
7)	Nozomi Saito, Yoshitomo Suhara, Masaaki Kurihara, Toshie Fujishima, Shinobu Honzawa, Hitoshi Takayanagi, Toshiro Kozono, Masahiko Matsumoto, Masayuki Ohmori, <u>Naoki Miyata</u> , Hiroaki Takayama, Atsushi Kittaka,	Design and efficient synthesis of 2 $\alpha$ -( $\omega$ -hydroxy)-1 $\alpha$ ,25-dihydroxyvitamin D3 analogues, including 2- <i>epi</i> -ED-71 and their 20-epimers with HL-60 cell differentiation activity	<i>J. Org. Chem.</i>	69(22)	7463-7471	2004
8)	Mariko Murata, Shiho Ohnishi, Kazuharu Seike, Kiyoshi Fukuhara, <u>Naoki Miyata</u> , Shosuke Kawanishi	Oxidative DNA damage induced by carcinogenic dinitropyrenes in the presence of P450 reductase	<i>Chem. Res. Toxicol.</i>	17(12)	1750-1756	2004
9)	Yasuhiro Noda, Tomoe Sumino, Yuki Fujisawa, <u>Naoki Miyata</u> , Toyo Kaiya, Kohfuku Kohda	1-Amino-4-phenyl-1,2,3,6-tetrahydro- pyridine and 1-amino-4-phenylpyridinium salt, the 1-amino analogues of neurotoxins, MPTP and MPP+, induce apoptosis in PC12 cells: Detection of apoptotic cells by comet assay and flow cytometric analysis	<i>In vivo</i>	18	561-569	2004

	発表者氏名	論文タイトル名	発表誌名	巻名	ページ	出版年
10)	Nobuyuki Sera, Hiroshi Tokiwa, Hideo Utsumi, Shigeki Sasaki, Kiyoshi Fukuhara, <u>Naoki Miyata</u>	Associations between chemical properties and oxidative damage due to nitrophenanthrenes and their related compounds in primary rat hepatocytes	<i>Polycyclic Aromatic Compounds</i>	24(4-5)	487-500	2004
11)	Masayuki Tanno, Shoko Sueyoshi, Kiyoshi Fukuhara, <u>Naoki Miyata</u> , <u>Haruhiro Okuda</u>	NO-release ability and DNA-damage activity of aromatic N-nitroso compounds	<i>Bull. of National Institute of Health Sciences</i>	122	10-15	2004
12)	I. Nakanishi, T. Kawashima, K. Ohkubo, H. Kanazawa, K. Inami, M. Mochizuki, K. Fukuhara, <u>H. Okuda</u> , T. Ozawa, S. Itoh, S. Fukuzumi, and N. Ikota	Electron-Transfer Mechanism in Radical-Scavenging Reactions by a Vitamin E Model in a Protic Medium	<i>Org. Biomol. Chem</i>	3	626-629	2005
13)	I. Nakanishi, K. Ohkubo, K. Miyazaki, W. Hakamata, S. Urano, T. Ozawa, <u>H. Okuda</u> , S. Fukuzumi, N. Ikota, and K. Fukuhara	A planar catechin analogue having a more negative oxidation potential than (+)-catechin as an electron-transfer antioxidant against a peroxy Radical	<i>Chem. Res. Toxicol.</i>	17	26-31	2004
14)	Yamada K, <u>Suzuki T</u> , Kohara A, Hayashi M, Mizutani T, Saeki K	In vivo mutagenicity of benzo[f]quinoline, benzo[h]quinoline, and 1,7-phenanthroline using the lac Z transgenic mice	<i>Mutation Research</i>	559	83-95	2004
15)	Arlt VM, Zhan L, Schmeiser HH, Honma M, Hayashi M, Phillips DH, <u>Suzuki T</u>	DNA adducts and mutagenic specificity of the ubiquitous environmental pollutant 3-nitrobenzanthrone in Muta Mouse	<i>Environ. Mol. Mutagen.</i>	43	186-195	2004
16)	鈴木孝禎、 <u>宮田直樹</u>	ヒストン脱アセチル化酵素阻害剤開発の最前線	ファルマシア	41	<i>in press</i>	2005
17)	鈴木孝禎、中川秀彦、 <u>宮田直樹</u>	癌の分子標的治療薬の開発:非ヒドロキサム酸系ヒストン脱アセチル化酵素阻害薬の設計、合成と生物活性評価	有機合成化学協会誌	63	<i>in press</i>	2005

**IV. 研究成果の刊行物・別刷**  
**(平成16年度)**

# Novel Inhibitors of Human Histone Deacetylases: Design, Synthesis, Enzyme Inhibition, and Cancer Cell Growth Inhibition of SAHA-Based Non-hydroxamates

Takayoshi Suzuki,<sup>\*,†</sup> Yuki Nagano,<sup>†</sup> Akiyasu Kouketsu,<sup>†</sup> Azusa Matsuura,<sup>†</sup> Sakiko Maruyama,<sup>‡</sup> Mineko Kurotaki,<sup>‡</sup> Hidehiko Nakagawa,<sup>†</sup> and Naoki Miyata<sup>\*,†</sup>

Graduate School of Pharmaceutical Sciences, Nagoya City University, 3-1 Tanabe-dori, Mizuho-ku, Nagoya, Aichi 467-8603, Japan, and Evaluation Group, Drug Research Department, R. & D. Division, Pharmaceuticals Group, Nippon Kayaku Co., Ltd., 31-12, Shimo 3-chome, Kita-ku, Tokyo 115-8588, Japan

Received October 1, 2004

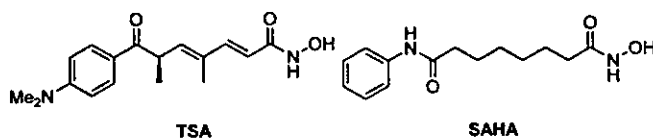
To find novel non-hydroxamate histone deacetylase (HDAC) inhibitors, a series of compounds modeled after suberoylanilide hydroxamic acid (SAHA) was designed and synthesized. In this series, compound **7**, in which the hydroxamic acid of SAHA is replaced by a thiol, was found to be as potent as SAHA, and optimization of this series led to the identification of HDAC inhibitors more potent than SAHA. In cancer cell growth inhibition assay, *S*-isobutyryl derivative **51** showed strong activity, and its potency was comparable to that of SAHA. The cancer cell growth inhibitory activity was verified to be the result of histone hyperacetylation and subsequent induction of p21<sup>WAF1/CIP1</sup> by Western blot analysis. Kinetic enzyme assay and molecular modeling suggest the thiol formed by enzymatic hydrolysis within the cell interacts with the zinc ion in the active site of HDACs.

## Introduction

The reversible acetylation of the  $\epsilon$ -amino groups of specific histone lysine residues by histone deacetylases (HDACs) and histone acetyl transferases is an important regulatory mechanism of gene expression.<sup>1</sup> When HDACs are inhibited, histone hyperacetylation occurs. The disruption of the chromatin structure by histone hyperacetylation leads to the transcriptional activation of a number of genes.<sup>2</sup> One important outcome of the activation is induction of the cyclin-dependent kinase inhibitory protein p21<sup>WAF1/CIP1</sup>, which causes cell cycle arrest.<sup>3</sup> Indeed, HDAC inhibitors such as trichostatin A (TSA) and suberoylanilide hydroxamic acid (SAHA) (Chart 1) have been reported to inhibit cell growth, induce terminal differentiation in tumor cells,<sup>4</sup> and prevent the formation of malignant tumors in mice.<sup>5</sup> Therefore, HDACs have emerged as attractive targets in anticancer drug development, and HDAC inhibitors have also been viewed as useful tools to study the function of these enzymes.

Many groups have ongoing research programs to find nonpeptide small-molecule inhibitors of HDACs, and these efforts have led to the identification of several classes of inhibitors.<sup>6</sup> Most previously reported HDAC inhibitors belong to hydroxamic acid derivatives, typified by TSA and SAHA, which are thought to chelate the zinc ion in the active site in a bidentate fashion through its CO and OH groups.<sup>7</sup> However, hydroxamic acids occasionally have been associated with problems such as poor pharmacokinetics and severe toxicity.<sup>8</sup> Thus, it has become increasingly desirable to find

Chart 1



replacements that possess strong inhibitory action against HDACs. In addition, in terms of biological research, the discovery of novel zinc-binding groups (ZBGs) may lead to a new type of HDAC isozyme-selective inhibitors which are useful as tools for probing the biology of the enzyme.<sup>9</sup> Thus far, *o*-aminoanilide,<sup>9,10</sup> electrophilic ketones,<sup>11</sup> and *N*-formyl hydroxylamine<sup>12</sup> have been reported as ZBGs in small-molecule HDAC inhibitors. However, most of them have reduced potency as compared to hydroxamic acid, and unfortunately, HDAC inhibitors bearing electrophilic ketones<sup>11</sup> have a metabolic disadvantage in that they are readily reduced to inactive alcohols *in vivo*, even within cells. We therefore initiated a search for replacement groups for hydroxamic acid with the goal of drug discovery as well as finding new tools for biological research, and found some potent non-hydroxamate small-molecule HDAC inhibitors.<sup>13</sup> We now present a full account of our study reporting the design, synthesis, HDAC inhibition, cancer cell growth inhibition, and binding mode analysis of non-hydroxamates based on the structure of SAHA.

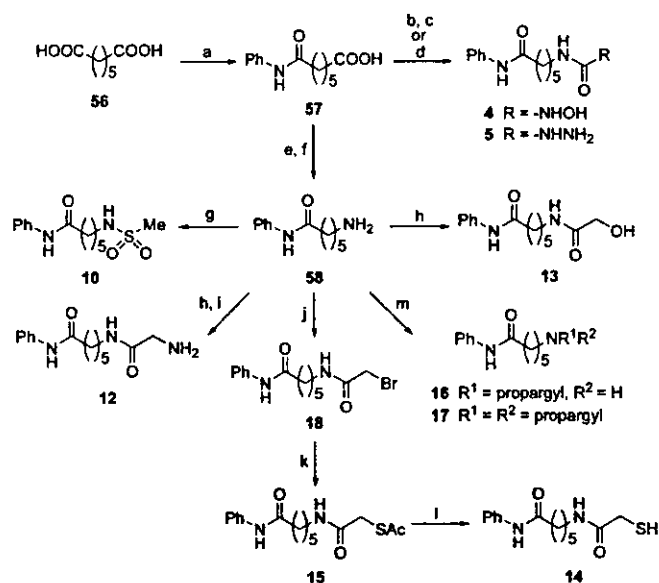
## Chemistry

The compounds prepared for this study are shown in Tables 1–5. The routes used for synthesis of the compounds are shown in Schemes 1–4. Scheme 1 shows the preparation of compounds **4**, **5**, **10**, **12–17**, and **18**. Compounds **4** and **5** were synthesized from pimelic acid **56**. The condensation of pimelic acid **56** with an equiva-

\* To whom correspondence should be addressed. Tel and fax: +81-52-836-3407; e-mail: miyata-n@phar.nagoya-cu.ac.jp; suzuki@phar.nagoya-cu.ac.jp

<sup>†</sup> Graduate School of Pharmaceutical Sciences, Nagoya City University.

<sup>‡</sup> Nippon Kayaku Co., Ltd.

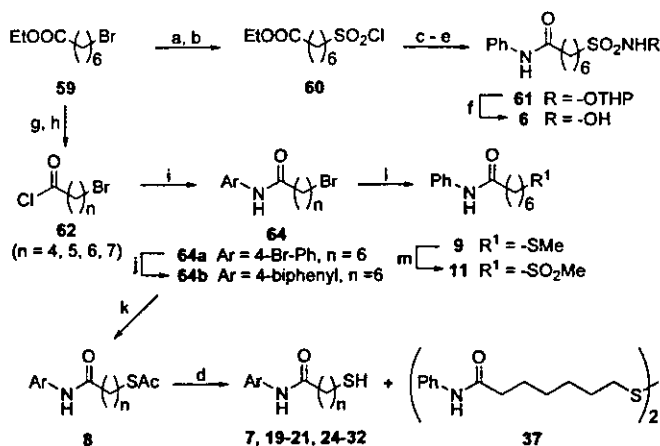
Scheme 1<sup>a</sup>

<sup>a</sup> Reagents and conditions: (a) aniline, 180 °C; (b) diphenylphosphoryl azide (DPPA), Et<sub>3</sub>N, toluene, reflux, and then *O*-(2-tetrahydropyranyl)hydroxylamine, reflux; (c) TsOH, MeOH, rt; (d) DPPA, Et<sub>3</sub>N, benzene, reflux, and then hydrazine monohydrate, reflux; (e) DPPA, Et<sub>3</sub>N, benzene, reflux, and then BnOH, reflux; (f) H<sub>2</sub>, 5% Pd-C, MeOH, rt; (g) MsCl, pyridine, rt; (h) HOCH<sub>2</sub>COOH or BocNHCH<sub>2</sub>COOH, EDCI, HOBT, DMF, rt; (i) TFA, CHCl<sub>3</sub>, rt; (j) BrCH<sub>2</sub>COBr, Et<sub>3</sub>N, THF, rt; (k) AcSK, EtOH, rt; (l) K<sub>2</sub>CO<sub>3</sub>, MeOH, rt; (m) propargyl bromide, K<sub>2</sub>CO<sub>3</sub>, MeOH, rt.

lent amount of aniline gave mono-anilide **57**. Curtius rearrangement of the acyl azide prepared from carboxylic acid **57** using diphenylphosphoryl azide provided the isocyanates, which on treatment with *O*-tetrahydropyranyl (THP) hydroxylamine or hydrazine gave *O*-THP hydroxyurea and semicarbazide **5**. Deprotection of the THP group of the *O*-THP hydroxyurea under acidic conditions afforded hydroxyurea **4**.

Compounds **10**, **12**–**17**, and **18** were prepared from carboxylic acid **57** obtained above via amine **58** by the procedure outlined in Scheme 1. Carboxylic acid **57** was converted to amine **58** with a three-step sequence: Curtius rearrangement of the acyl azide prepared from carboxylic acid **57**, treatment of the resulting isocyanates with benzyl alcohol, and removal of the Z group by hydrogenation. Coupling between amine **58** and methanesulfonyl chloride afforded sulfonamide **10**. The reaction of amine **58** with *N*-Boc glycine in the presence of EDCI and HOBT in DMF was followed by treatment with trifluoroacetic acid to give aminoacetamide **12**. Hydroxyacetamide **13** was obtained in one step using the procedure described for **12**. The amino group of **58** was acylated with bromoacetyl bromide to yield bromoacetamide **18**. Bromide **18** was treated with potassium thioacetate to give thioacetate **15**, after which deacetylation of the thioacetate in the presence of K<sub>2</sub>CO<sub>3</sub> in MeOH gave mercaptoacetamide **14**. The amine **58** was allowed to react with propargyl bromide in the presence of K<sub>2</sub>CO<sub>3</sub> to give mono- and di-alkylated compounds **16** and **17**.

Compounds **6**–**9**, **11**, **19**–**21**, **24**–**32**, and **37** were prepared from another starting material, **59** (Scheme 2). The preparation of hydroxysulfonamide **6** was achieved via sulfonyl chloride **60**. Bromide **59** was converted to sulfonyl chloride **60** by sulfation and by a

Scheme 2<sup>a</sup>

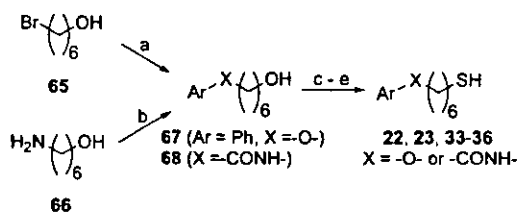
<sup>a</sup> Reagents and conditions: (a) Na<sub>2</sub>SO<sub>3</sub>, EtOH, H<sub>2</sub>O, reflux; (b) SOCl<sub>2</sub>, DMF, toluene, reflux; (c) *O*-(2-tetrahydropyranyl)hydroxylamine, 4-(dimethylamino)pyridine, pyridine, CH<sub>2</sub>Cl<sub>2</sub>, rt; (d) 2N aq NaOH, EtOH, rt; (e) aniline, EDCI, HOBT, DMF, rt; (f) TFA, CH<sub>2</sub>Cl<sub>2</sub>, 60 °C; (g) LiOH·H<sub>2</sub>O, EtOH, THF, H<sub>2</sub>O, rt; (h) (COCl)<sub>2</sub>, DMF, CH<sub>2</sub>Cl<sub>2</sub>, rt; (i) ArNH<sub>2</sub> (**63**), Et<sub>3</sub>N, CH<sub>2</sub>Cl<sub>2</sub>, rt; (j) PhB(OH)<sub>2</sub>, Pd(PPh<sub>3</sub>)<sub>4</sub>, NaHCO<sub>3</sub>, 1-methyl-2-pyrrolidinone, H<sub>2</sub>O, 80 °C; (k) AcSK, EtOH, rt; (l) 15% aq NaSMe, EtOH, rt; (m) *m*-chloroperoxybenzoic acid, CH<sub>2</sub>Cl<sub>2</sub>, rt.

subsequent reaction with thionyl chloride. The sulfonyl chloride **60** was treated with *O*-THP hydroxylamine to give *O*-THP hydroxysulfonamide, after which hydrolysis of the ester under alkaline conditions and subsequent amide formation with aniline gave compound **61**. Removal of the THP group of compound **61** by treatment with trifluoroacetic acid gave hydroxysulfonamide **6**.

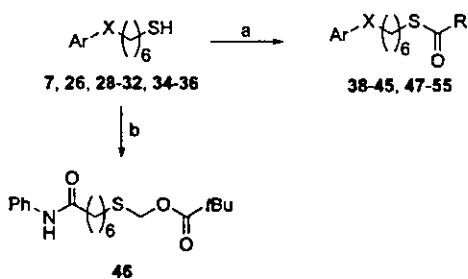
Compounds **7**–**9**, **11**, **19**–**21**, **24**–**32**, and **37** were synthesized from the corresponding acid chlorides **62** (**62a** (*n* = 4) and **62b** (*n* = 5) are commercially available) by the route shown in Scheme 2. **62c** (*n* = 6) was prepared from ester **59** by hydrolysis of the ethyl ester and a subsequent reaction with oxalyl chloride, and **62d** (*n* = 7) was obtained in the same way as **62c**. The amino group of aromatic amines **63** was acylated with an appropriate acid chloride **62** to give the amides **64**. Suzuki coupling<sup>14</sup> of bromobenzene **64a** with phenylboronic acid provided the biphenyl **64b**. Bromides **64** were treated with potassium thioacetate to give compound **8**, after which hydrolysis of the thioacetates under alkaline conditions gave the desired compounds **7**, **19**–**21**, **24**–**31**, and **32**, and disulfide **37** was obtained as a byproduct when thiol **7** was synthesized. Sulfide **9** was prepared by the alkylation of methylmercaptan with bromide **64c** (Ar = Ph, *n* = 6). Oxidation of **9** with 2 equiv of *m*-chloroperoxybenzoic acid provided the sulfone **11**.

Thiols **22**, **23**, **33**–**35**, and **36** were prepared from alcohol **65** or **66** by the procedure outlined in Scheme 3. Treatment of bromide **65** with phenol in the presence of K<sub>2</sub>CO<sub>3</sub> gave ether **67**, and condensation of amine **66** with an appropriate aromatic carboxylic acid **69** afforded amides **68**. Alcohols **67** and **68** were converted to thiols **22**, **23**, **33**–**35**, and **36** in three steps by conversion of the alcohols to bromides, treatment of the bromides with potassium thioacetate, and hydrolysis of the resulting thioacetates.

The preparation of *S*-chemically modified compounds **38**–**54**, and **55** is shown in Scheme 4. Thiols **7**, **26**, **28**–**32**, **34**, **35**, and **36** were coupled with the corresponding

Scheme 3<sup>a</sup>

<sup>a</sup> Reagents and conditions: (a) Phenol, K<sub>2</sub>CO<sub>3</sub>, DMF, 80 °C; (b) ArCOOH (69), EDCI, HOBT, DMF, rt; (c) CBr<sub>4</sub>, PPh<sub>3</sub>, CH<sub>2</sub>Cl<sub>2</sub>, 0 °C; (d) AcSK, EtOH, rt; (e) 2N aq NaOH, EtOH, THF, rt.

Scheme 4<sup>a</sup>

<sup>a</sup> Reagents and conditions: (a) RCOCl (70), 4-(dimethylamino)pyridine, pyridine, CH<sub>2</sub>Cl<sub>2</sub>, rt; (b) NaH, chloromethyl pivalate, DMF, 0 °C to room temperature.

acyl chloride **70** to give thioesters **38–45**, **47–54**, and **55**. Alkylation of thiol **7** with chloromethyl pivalate in the presence of sodium hydride in DMF afforded compound **46**.

## Results and Discussion

**Enzyme Assays.** The compounds synthesized in this study were tested with an *in vitro* assay using a HeLa nuclear extract rich in HDAC activity. The results are summarized in Tables 1–3.

The IC<sub>50</sub> values of SAHA and *o*-aminoanilide **1** were 0.28 μM and 120 μM, respectively (entries 1 and 2). α-Ketoamide **2** and *N*-formyl hydroxylamine **3** were reported previously to inhibit HDACs with an IC<sub>50</sub> of 0.34 μM and 2.8 μM, respectively (entries 3 and 4).<sup>11b,12</sup>

The crystal structures of an archaeobacterial HDAC homologue (HDAC-like protein, HDLP)/hydroxamates and HDAC8/hydroxamates complexes made it clear that the hydroxamic acid group coordinates the zinc ion in the active site through its CO and OH groups and also forms three hydrogen bonds between its CO, NH, and OH groups and Tyr 306, His 143, and His 142 (HDAC8 numbering), respectively.<sup>7</sup> From these data, hydroxyurea **4**, semicarbazide **5**, and hydroxysulfonamide **6** were synthesized and tested as HDAC inhibitors because it is possible for them to chelate zinc ion and form hydrogen bonds with Tyr and His like SAHA. Among these three compounds, hydroxyurea **4** and semicarbazide **5** showed anti-HDAC activity and the IC<sub>50</sub> values were comparable to that of *o*-aminoanilide **1** (entries 5, 6, and 7). However, they were much less effective than SAHA.

Thiols seemed to be reasonable targets for hydroxamic acid replacements, because zinc ion is highly thiophilic and thiol derivatives have been reported to inhibit zinc-dependent enzymes such as angiotensin converting enzyme<sup>15</sup> and matrix metalloproteinases.<sup>16</sup> Furthermore, macrocyclic compounds bearing a disulfide group such as FK228 have been reported recently to inhibit

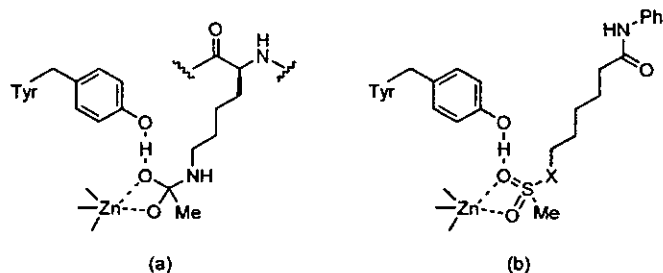


**Figure 1.** The transition state proposed for HDACs (a), and models for the binding of sulfone derivatives (b).

HDACs under reductive conditions.<sup>17</sup> Surprisingly, although the inhibitory ability of monodentate ZBGs such as thiol was thought to be less than that of bidentate ZBGs such as hydroxamate, *N*-formyl hydroxylamine, and hydrated electrophilic ketones,<sup>16</sup> the activity of thiol **7** was far greater than expected. A pronounced inhibitory effect (IC<sub>50</sub> = 0.21 μM) was observed with thiol **7**, which was much more active than previously reported non-hydroxamates such as *o*-aminoanilide, *N*-formyl hydroxylamine, and trifluoromethyl ketone,<sup>11a</sup> and as potent as α-ketoamide **2** and SAHA (entry 8). To confirm that the thiol group plays an important role in anti-HDAC activity, thioacetate **8a** and methyl sulfide **9** were tested. As expected, thiol transformation into thioacetate and methyl sulfide led to an inhibitor that was about 30-fold less potent and a compound devoid of anti-HDAC activity, respectively (entries 9 and 10). These results suggest that thiolate anion generated under physiological conditions has an intimate involvement in the interaction with the zinc ion in the active site.

The crystal structures of the HDLP/hydroxamates and HDAC8/hydroxamates complexes have led to a solid understanding of not only the three-dimensional structure of the active site of HDACs but also the catalytic mechanism for the deacetylation of acetylated lysine substrate.<sup>7</sup> It has been proposed that the carbonyl oxygen of this substrate could bind the zinc, and the carbonyl could be attacked by a zinc-chelating water molecule (Figure 2a), which would result in the production of deacetylated lysine via a tetrahedral carbon-containing transition state (Figure 1a). On the basis of the proposed catalytic mechanism, we attempted to design non-hydroxamate HDAC inhibitors. First, we designed transition-state (TS) analogues. The TS of HDAC deacetylation was estimated to include a tetrahedral carbon (Figure 1a) as with other zinc proteases.<sup>18</sup> We focused attention on sulfone derivative TS analogues because it has been suggested that the sulfonamide moiety has strong similarity with the TS of amide bond hydrolysis, both from a steric and an electronic point of view.<sup>19</sup> Compounds **10** and **11**, in which a hydroxamic acid of SAHA is replaced by a sulfonamide and a sulfone, respectively, were designed and synthesized as TS analogues (Figure 1b). Of these two TS analogues, sulfone **11** showed anti-HDAC activity and the IC<sub>50</sub> value was 230 μM (entries 11 and 12). However, sulfone **11** was approximately 820-fold less effective than SAHA.

Our next approach was based on the proposed deacetylation mechanism whereby a zinc-chelating water molecule activated by His142 and His 143 (HDAC8 numbering) makes a nucleophilic attack on the carbonyl carbon of an acetylated lysine substrate (Figure 2a).

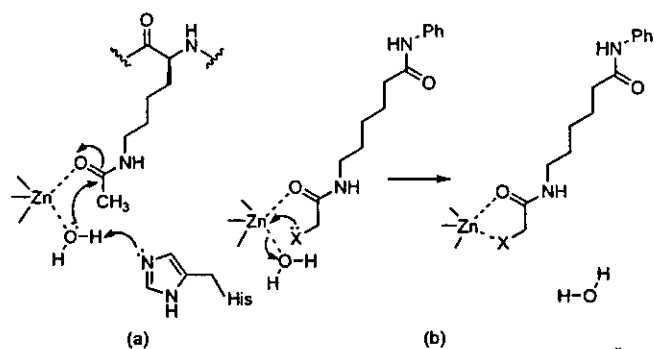


**Figure 2.** The mechanism proposed for the deacetylation of acetylated lysine substrate (a), and a model for the binding of heteroatom-containing substrate analogues to zinc ion (b).

**Table 1.** HDAC Inhibition Data for SAHA and SAHA-based Non-hydroxamates<sup>a</sup>

entry	compd	R	n	% inhibtn at 100 $\mu$ M	IC <sub>50</sub> ( $\mu$ M)
1	SAHA <sup>b</sup>	-CONHOH	6	100	0.28
2	1 <sup>c</sup>		6	48	120
3	2	-COCONHMe	6	ND	0.34 <sup>d</sup>
4	3		7	ND	2.8 <sup>e</sup>
5	4	-NHCONHOH	5	58	80
6	5	-NHCONHNH <sub>2</sub>	5	35	150
7	6	-SO <sub>2</sub> NHOH	6	14	>100
8	7	-SH	6	100	0.21
9	8a	-SAc	6	85	7.1
10	9	-SMe	6	11	>100
11	10	-NHSO <sub>2</sub> Me	5	10	7500
12	11	-SO <sub>2</sub> Me	6	33	230
13	12 <sup>f</sup>	-NHCOCH <sub>2</sub> NH <sub>2</sub>	5	6	>100
14	13	-NHCOCH <sub>2</sub> OH	5	0	>100
15	14	-NHCOCH <sub>2</sub> SH	5	99	0.39
16	15	-NHCOCH <sub>2</sub> SAc	5	72	22
17	16		5	14	>100
18	17		5	0	>100
19	18	-NHCOCH <sub>2</sub> Br	5	78	17

<sup>a</sup> Values are means of at least three experiments. <sup>b</sup> Prepared as described in ref 26. <sup>c</sup> Prepared as described in ref 9a. <sup>d</sup> Data taken from the literature (ref 11b). <sup>e</sup> Data taken from the literature (ref 12). <sup>f</sup> Trifluoroacetic acid salt. ND = No data.

With this mechanism, if the water molecule is forcibly removed from the zinc ion, the HDACs would supposedly be inhibited. We then designed and synthesized heteroatom-containing substrate analogues 12, 13, and 14. These analogues would be recognized as substrates by HDACs and would be easily taken into the active site where they could force the water molecule off the zinc ion and the reactive site for the deacetylation by chelation of the heteroatom to the zinc ion, and might behave as HDAC inhibitors (Figure 2b). As shown in Table 1 (entries 13, 14, and 15), potent inhibition was observed with mercaptoacetamide 14, while 12 and 13 did not possess HDAC inhibitory activities. Mercaptoacetamide 14 exhibited an IC<sub>50</sub> of 0.39  $\mu$ M, and its activity largely surpassed those of *o*-aminoanilide 1 and *N*-formyl hydroxylamine 3 and was comparable to those of  $\alpha$ -ketoamide 2 and SAHA. As expected, thiol trans-

**Table 2.** Effect of Linker Variation on HDAC Inhibitory Activity of Thiols<sup>a</sup>

entry	compd	X	n	IC <sub>50</sub> ( $\mu$ M)
1	7	-NHCO-	6	0.21
2	19	-NHCO-	7	1.5
3	20	-NHCO-	5	0.37
4	21	-NHCO-	4	6.2
5	22	-O-	6	11
6	23	-CONH-	6	0.36

<sup>a</sup> Values are means of at least three experiments.

**Table 3.** Effect of Aromatic Group Variation on HDAC Inhibitory Activity of Thiols<sup>a</sup>

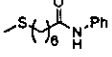
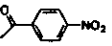
entry	compd	Ar	X	IC <sub>50</sub> ( $\mu$ M)
1	7	-Ph	-NHCO-	0.21
2	24		-NHCO-	1.2
3	25		-NHCO-	1.1
4	26		-NHCO-	0.075
5	27		-NHCO-	0.62
6	28		-NHCO-	0.21
7	29		-NHCO-	0.11
8	30		-NHCO-	0.072
9	31		-NHCO-	0.17
10	32		-NHCO-	0.34
11	23	-Ph	-CONH-	0.36
12	33		-CONH-	0.61
13	34		-CONH-	0.085
14	35		-CONH-	0.079
15	36		-CONH-	0.10

<sup>a</sup> Values are means of at least three experiments.

formation into thioacetate (15) led to a 55-fold less potent inhibitor. This result suggests the ease of ionization of thiol is an important factor for HDAC inhibition like the case of thiol 7.

We turned our attention to irreversible HDAC inhibitors. TPX B is an irreversible HDAC inhibitor,<sup>20</sup> and finding more specific and simpler irreversible HDAC inhibitors is useful for the isolation and cloning of an HDAC.<sup>2</sup> As described above, the crystal structures of the HDLP/hydroxamates and HDAC8/hydroxamates complexes revealed that the hydroxamic acid group forms three hydrogen bonds with Tyr 306, His 143, and His 142, and furthermore, zinc ion is coordinated by His 180, Asp 178, and Asp 267 (HDAC8 numbering). Since the phenol group of Tyr, the imidazole group of His, and the carboxyl group of Asp are able to react with electrophiles, we prepared analogues bearing propargyl

**Table 4.** Cell Growth Inhibition Data on NCI-H460 Cells for Compound **7** and Its *S*-Modified Prodrugs<sup>a</sup>

Ph-X-(CH <sub>2</sub> ) <sub>n</sub> -S-R				
entry	compd	R	EC <sub>50</sub> (μM)	
1	7	-H	>50 <sup>b</sup>	
2	37		>50 <sup>c</sup>	
3	8a	-Ac	36	
4	38	-COEt	28	
5	39	-CO <sup><i>n</i></sup> -Pr	22	
6	40	-CO <sup><i>n</i></sup> -Pr	20	
7	41	-CO <sup><i>n</i></sup> -Bu	>50 <sup>d</sup>	
8	42		27	
9	43		21	
10	44	-Bz	25	
11	45		24	
12	46	-CH <sub>2</sub> OCOR-Bu	25	

<sup>a</sup> Values are means of at least two experiments. <sup>b</sup> 34% inhibition at 50 μM. <sup>c</sup> 10% inhibition at 50 μM. <sup>d</sup> 42% inhibition at 50 μM.

amino (**16**, **17**) and bromoacetamide (**18**) which could form covalent bonds with Tyr, His, and Asp of the enzyme, and evaluated their anti-HDAC activities. While propargyl amino compounds **16** and **17** did not possess HDAC inhibitory activities, more potent inhibition was observed with bromoacetamide **18** (entries 17, 18, and 19). Bromoacetamide **18** exhibited an IC<sub>50</sub> of 17 μM and its activity was about 9-fold as strong as that of *o*-aminoanilide **1**, but much weaker than that of SAHA.

With the results shown in Table 1, we were encouraged to study further the structure-activity relationship (SAR) and structural optimization. We selected thiol **7** for further study.<sup>21</sup> First, we examined the effect of linker parts of thiol **7**. The results are summarized in Table 2. HDAC inhibition was distinctly dependent on chain length, with *n* = 7 (**19**) and *n* = 4 (**21**) resulting in less potent inhibitors. However, compound **20**, in which *n* = 5, showed essentially the same potency as compound **7**, in which *n* = 6 (entries 1–4). The similar SAR between thiols and hydroxamates, with *n* = 6 optimal,<sup>22</sup> indicates that thiols inhibit HDACs in a binding mode similar to that of hydroxamates. As for the group attaching the phenyl moiety, ether **22** displayed moderate activity, whereas the activity of the reversed amide **23** was maintained (entries 5 and 6).

Next, the aromatic group was examined (Table 3). In the amide-linked series (entries 1–10), 4-substituted phenyl compounds tended to decrease the potency. Specifically, compounds **24** (Ar = 4-NMe<sub>2</sub>-Ph), **25** (Ar = 4-biphenyl), and **27** (Ar = 4-PhO-Ph) showed about a 3- to 6-fold decrease in potency when compared to the parent thiol **7** (entries 2, 3, and 5). On the other hand, compound **26**, in which a phenyl group was introduced at the 3-position of the phenyl group of **7**, showed 3-fold increased inhibitory activity (IC<sub>50</sub> of 0.075 μM, entry 4). In addition, 3-phenoxy compound **28** was equipotent with compound **7** (entry 6). We investigated the effect of the replacement of the phenyl group of compound **7** with heteroaryl rings (entries 7, 8, 9, and 10). Changing the benzene ring to a 3-pyridine ring (**29**), 4-phenyl-2-thiazole ring (**31**), and 2-benzothiazole ring (**32**) sus-

**Table 5.** Cell Growth Inhibition Data on NCI-H460 Cells for Compound **40** and Its Derivatives<sup>a</sup>

Ar-X-(CH <sub>2</sub> ) <sub>n</sub> -S-CO-CH(CH <sub>3</sub> ) <sub>2</sub>					
entry	compd	Ar	X	EC <sub>50</sub> (μM)	
1	40	-Ph	-NHCO-	20	
2	47		-NHCO-	2.8	
3	48		-NHCO-	25	
4	49		-NHCO-	2.9	
5	50		-NHCO-	8.0	
6	51		-NHCO-	2.1	
7	52		-NHCO-	9.5	
8	53		-CONH-	12	
9	54		-CONH-	4.1	
10	55		-CONH-	12	

<sup>a</sup> Values are means of at least two experiments.

**Table 6.** Growth Inhibition of Various Cancer Cells Using SAHA and Compound **51**<sup>a</sup>

	cell	SAHA, EC <sub>50</sub> (μM)	51, EC <sub>50</sub> (μM)
MDA-MB-231	breast cancer	1.5	2.3
SNB-78	central nervous system	16	9.1
HCT116	colon cancer	0.58	3.0
NCI-H226	lung cancer	2.6	2.6
LOX-IMVI	melanoma	1.3	1.1
SK-OV-3	ovarian cancer	2.5	4.5
RXF-631L	renal cancer	2.0	2.4
St-4	stomach cancer	5.2	5.0
DU-145	prostate cancer	1.6	4.5
	mean	3.7	3.8

<sup>a</sup> Values are means of at least two experiments.

tained or slightly reduced the activity, whereas quinoline **30** had improved activity (IC<sub>50</sub> of 0.072 μM), and turned out to be the most potent compound in this series. The reverse amide-linked series (entries 11–15) exhibited potencies similar to or greater than the parent thiol **23**, with the exception of **33** (Ar = 4-NMe<sub>2</sub>-Ph), which resulted in a slightly less potent inhibitor. In particular, the reversed amides **34** with a naphthalene substituent and **35** with a benzofuran substituent exhibited about 3-fold increases in potency (IC<sub>50</sub>s of 0.085 μM and 0.079 μM, respectively). As a result, IC<sub>50</sub>s in the double-digit nanomolar range were observed with 3-biphenyl **26**, quinoline **30**, naphthalene **34**, and benzofuran **35**, which were approximately 3- to 4-fold more potent than SAHA.

**Cancer Cell Growth Inhibition Assay.** To confirm the effectiveness of thiol-based HDAC inhibitors as anticancer drugs and tools for biological research, thiol **7** was initially tested in a cancer cell growth inhibition